

OPTICAL SYSTEM DESIGN

R. E. English, Jr. J. Miller
C. Laumann L. Seppala

The optical system for the NIF includes every performance-based piece of glass in the system: many thousands of mirrors, lenses, amplifier slabs, polarizers, crystals, windows, diffractive optics plates, etc. This complex system is divided into six subsystems, each with its own requirements and design issues. In Title I, we have completed preliminary designs for each subsystem. Specifications are well beyond Title I requirements for the large-aperture optics, and we expect to start the procurement process for these optics early in Title II. This section will discuss those ~7000 large-aperture components. Optical design of the 15,000 to 20,000 smaller components will be treated briefly in discussions of specific subsystems.

Introduction

The optical system for the NIF encompasses every performance-based piece of glass in the entire system, including over 7000 pieces with large apertures (Table 1), the 5000 to 10,000 smaller optical components in the front-end of the laser system, and the several thousand small components in the beam alignment and control systems. We divide this system into six areas, as shown in Figure 1:

- The optical pulse generation system.
- The injection system.
- The main laser system.
- The switchyard and target area.
- The final optics assembly.
- The beam control systems.

The optical pulse generation system, injection system, and beam control systems contain smaller components that are in a preliminary state of design. These designs will be developed further in Title II. The preliminary designs for components in the opti-

cal pulse generation system and injection system are described in the “Laser Components” article of this Quarterly (p. 132). The component designs for the beam control systems are briefly discussed in “Laser Control Systems” (p. 180).

In this article, we describe the optical design and specifications of the large optical components comprising the main laser system, switchyard and target area, and final optics assembly. The optical configuration for these systems is contained in our configuration drawings, which detail the location, orientation, and size of

TABLE 1. NIF contains over 7000 large-aperture optics.

Component	Material	Number
Amplifier slabs	Laser glass	3072
Lenses	Fused silica	960
Deformable mirrors	BK-7	192
Cavity mirrors	BK-7	192
Elbow mirrors	BK-7	192
Transport mirrors	BK-7	816
Polarizers	BK-7	192
Crystals	KDP/KD*P	576
Debris shields	Fused silica	192
Switch windows	Fused silica	384
Vacuum windows	Fused silica	192
Diffractive optics plate	Fused silica	192
Total		7152

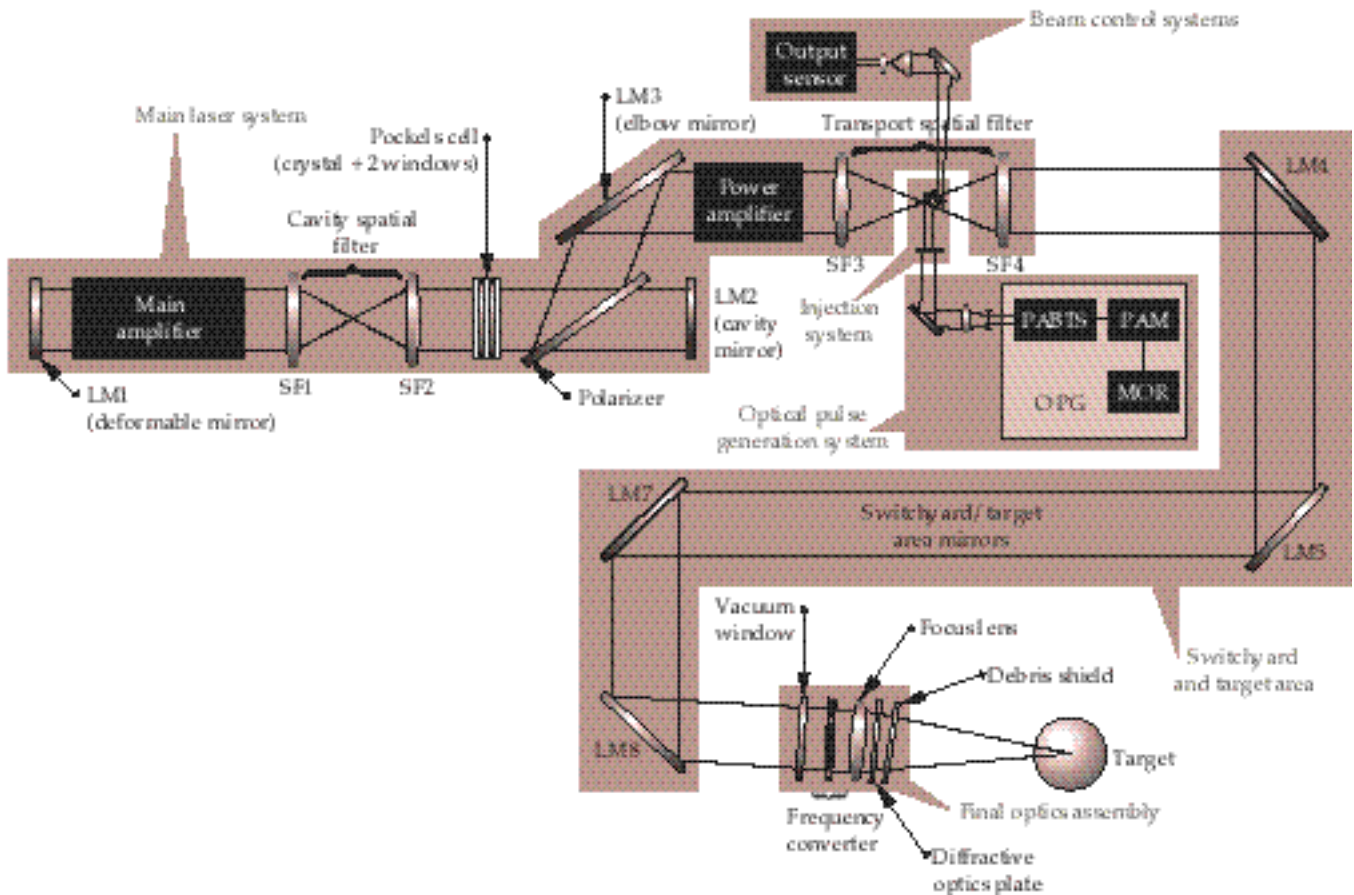


FIGURE 1. The six main optical systems (shaded areas) for the National Ignition Facility. (40-00-0997-2064pb01)

each NIF optical component. These components constitute a major fraction of the cost of the laser hardware and have a very long procurement lead time. The designs and specifications for these components are essentially complete, and we are ready to begin the procurement process. At the end of this section, we include a discussion of the specification process for the NIF large-aperture optics.

Main Laser System

In the main laser system, the large optical components include the amplifiers, the spatial filter, the periscope assembly, and the deformable mirror (Figure 2). In this section, we focus mostly on the optical design and components for the amplifiers and spatial filters, which are key to the design of the main laser. The basic features of the laser design come from laser physics optimization models—as discussed briefly in “Laser Requirements and Performance” (p. 99)—together with the practical

limits on the availability of large optics. At this time, the maximum practical clear aperture for the laser glass slabs used in the amplifiers, as well as for KDP crystals, is roughly 40 cm; we chose a clear aperture of 400×400 mm for the laser slabs. By definition, the amplifier is the limiting aperture in the main laser optical system. The laser optimization model shows that the best configuration to give us a wide operating range for the laser is to make these amplifier slabs 41 mm thick and place 11 in the main amplifier and 7 in the power amplifier. (As discussed in “Laser Requirements and Performance,” the cheaper 11-5 configuration has adequate performance, so we chose to build that configuration and leave space in the design to upgrade to the 11-7 configuration, if required.) The actual size of the slab is larger than the 400-mm clear aperture, since there are edge claddings on the slab to absorb amplified spontaneous emission and these become hot enough during laser pumping that a region of about a third to a half of the slab thickness around the edge is unusably

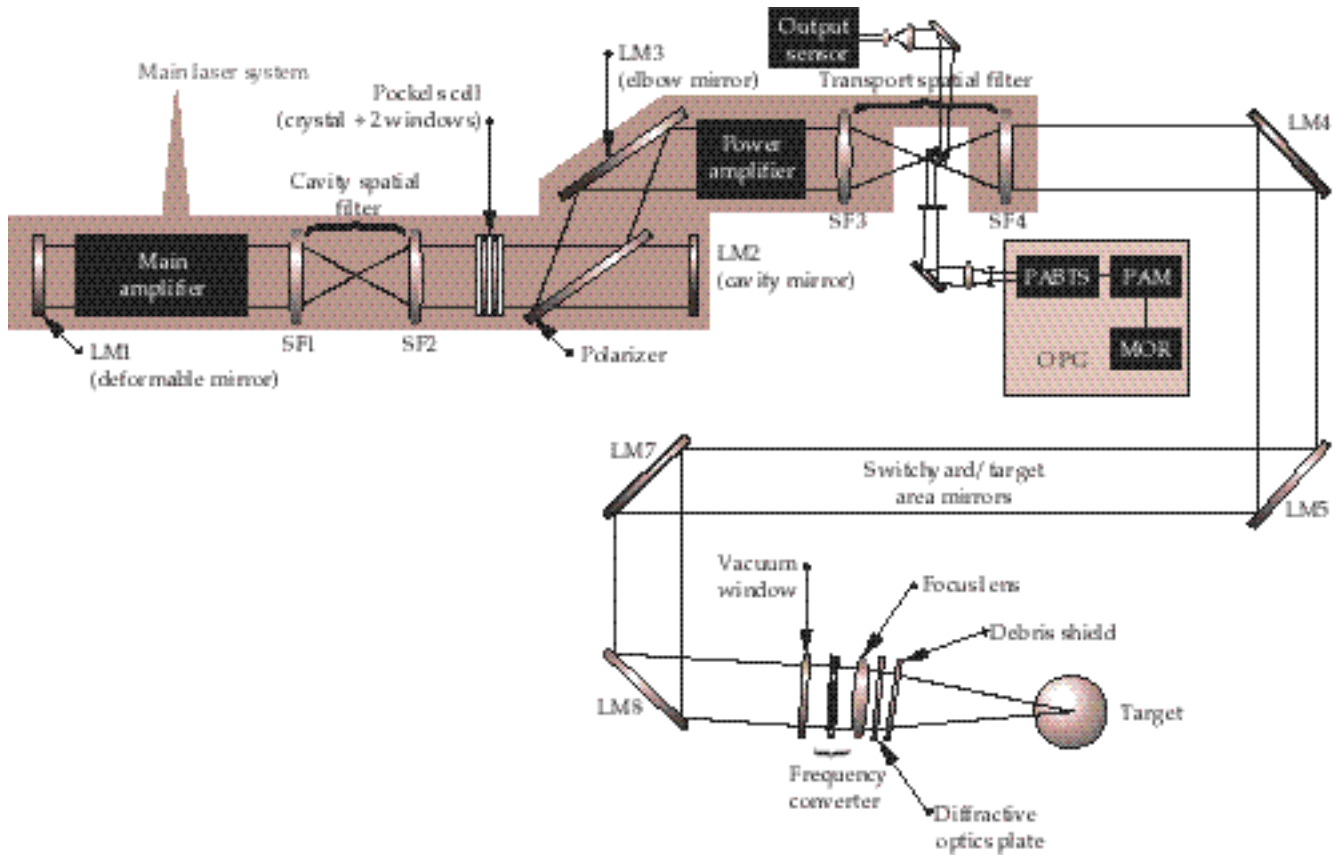


FIGURE 2. The main laser optical system. (40-00-0997-2065pb01)

distorted. The actual slab size, then, is 456.8×800.2 mm, including the edge cladding thickness. The slab is longer in one dimension because it is placed at Brewster's angle to the beam.

The cavity spatial filter (CSF) length is set by the length of the main amplifier, required ghost standoff distances, component access clearances, and the length of the periscope assembly. These components require a space of 23.5 m. Mirrors LM1 (the deformable mirror) and LM2 (the cavity mirror) both must lie at relay planes of the system, so the CSF length must also be 23.5 m, giving a cavity length of 47 m.

The transport spatial filter (TSF) must form an image of the relay plane near the frequency converters. An exact relay would require a TSF length of about 75 m, but a study with propagation codes shows that there is negligible increase in irradiance noise at the frequency converter for a 60-m-long TSF. We chose this shorter length to reduce cost.

The beams travel at a small angle to the optical axis, and this angle is set by the separation between the injection and output pinholes in the focal plane of the TSF. The required size of the injection mirror, plus necessary mechanical clearances, set a minimum spacing between these pinholes of 35 mm.

The diameter of these pinholes determines the angular content that we allow to propagate through the laser system, or the minimum spatial frequency of noise on the beam. This angle will vary to optimize performance for particular experiments over the range of ± 100 to $200 \mu\text{rad}$ (6 to 12 mm diameter in the TSF pinhole plane). The clear aperture required for each optical component in the laser falls out directly from these choices, with proper consideration for mounting and alignment tolerances.

The spatial filters are evacuated, so the spatial filter lenses serve as vacuum barriers, and this loading must be considered in the design. Also, the windows of the

Pockels cell must withstand a vacuum load. The Title I design presented here for these components has a maximum tensile stress of 700 psi, consistent with Nova experience. In Title II we shall evaluate the consequences of going to a lower-stress design (i.e., 500 psi), which requires slightly thicker components. The thickness of other components (mirrors and polarizers) is set to the minimum consistent with maintaining the acceptable flatness in the presence of mounting distortions and coating stress.

The maximum beam size is set by the aperture of the amplifier, the transverse motion of the beam in the cavity due to off-axis propagation (vignetting) and alignment and positioning tolerances. The vignetting allowance is ± 6 mm, and we allow ± 4 mm each for component placement and alignment. This gives a maximum beam size at zero intensity of 372×372 mm. The effective beam area (equivalent area assuming constant fluence across the beam) is about 1230 cm^2 , after allowing for the apodized edge region around the beam. This is slightly smaller than pre-Title I estimates because of revisions in component placement tolerances during Title I design.

The clear apertures of other components in the main laser are similarly set by beam size, and by vignetting, alignment, and placement allowances. Actual component dimensions are larger, as required for mounting. Table 2 summarizes the sizes of the main laser components.

Lenses SF1 and SF2 for the CSF are symmetric biconvex lenses with a very slight aspheric correction on one surface. The input lens to the TSF, SF3, is tilted with respect to the axis so that the backward single-reflection ghost (see “Ghost Beams in Large Laser Systems” on p. 116) strikes a beam dump outside the clear aperture of the beamline. This allows the distance between the power amplifier and SF3 to be shorter, saving space, but requires more aspheric correction. The output lens of the TSF, SF4, has an aspheric input surface and a flat output surface. This flat surface provides a diagnostic sample of the output beam for use by a wavefront sensor located near the TSF focal plane. The performance of these lenses, and the effect of the full laser beam propagation path through them, has been verified using the Code V® suite of optical design tools.

Title II Activities

High on the list of Title II optical design activities for the main laser system is to confirm our ghost management solutions. We will complete our ghost analysis, including tolerances, and specify locations for ghost reflection baffles and beam dumps in the main laser system. Also in Title II, we will complete the analysis for changing the lens thickness, based on a peak stress of 500 psi. We will also update the main laser optic system drawings to reflect minor adjustments in component locations and sizes.

TABLE 2. The sizes and apertures for the main laser large-aperture optics are under configuration control.

Optic	Name	Optical clear aperture (mm)	Mechanical hard aperture (mm)	Optics size (mm)
Amplifier slabs	Main/power amplifiers	400 × 400	401 × 401	800.2 × 456.8 × 41
CSF lens	SF1/2	406 × 406	409 × 409	434 × 434 × 46 ^a
TSF lens (input)	SF3	410 × 406	413 × 409	438 ^b × 434 × 46 ^a
TSF lens (output)	SF4	406 × 406	409 × 409	434 ^b × 434 × 46 ^a
Deformable mirror	LM1	392 × 392	392 × 392	449.5 × 433.7 × 10/30
Cavity mirror	LM2	392 × 392	392 × 392	412 × 412 × 80
Elbow mirror	LM3	396 × 392	397 × 393	417 × 740 ^b × 80
Polarizer	PL	396 × 396	397 × 397	417 × 807 ^b × 90
Switch crystal	SC	397 × 397	398 × 398	410 × 410 × 10
Switch window	SW	397 × 397	398 × 398	430 × 430 × 30 ^a

^a Lens thickness change pending approval by Level IV Change Control Board (ECR 66)

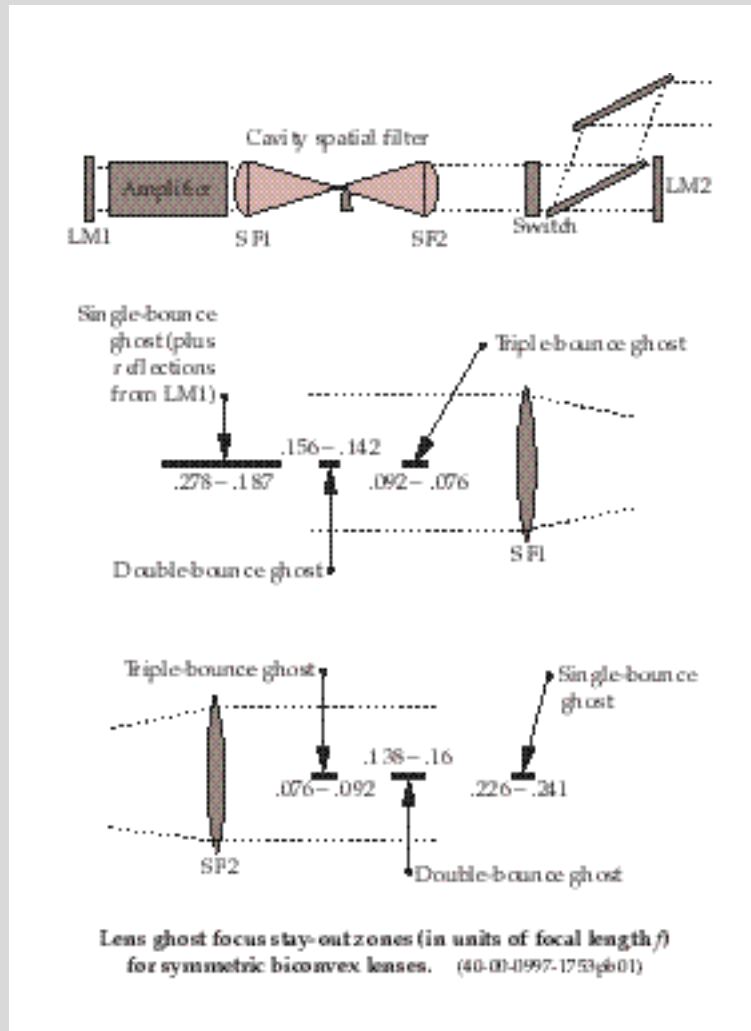
^b Dimensional changes pending approval by Level IV Change Control Board (ECR 69)

GHOST BEAMS IN LARGE LASER SYSTEMS

The surfaces of NIF transmissive optical components are all antireflection coated, but these coatings are never perfect. Each such surface reflects a small fraction of the incident beam, and this weak “ghost” beam propagates through the system. Even a small reflection of a high-energy beam can contain enough energy to damage optical components if those components lie near a position where the ghost beam comes to a focus. The ghost beams can also cause other difficulties. It is extremely important to manage where these beams fall in NIF.

The figure shows, as an example, the ghost reflections from symmetric biconvex lenses in the cavity spatial filter on NIF. A beam traveling from left to right through lens SF1 reflects from the second surface of the lens, propagates back towards the main amplifier, and comes to a focus at $0.233 f$ distance from the lens, where f is the lens focal length. If the reflectivity of this surface is 0.5%, the energy in this reflection can be as high as 50 J, and the ghost focus is a serious hazard to any optical component located in that vicinity. If one considers the size of the beam near focus, as well as multiple reflections between this lens and mirror LM1 (which must be considered, since they see the residual gain of the main amplifier), the hazardous zone extends from about 0.19 to $0.28 f$. For beams going from right to left through the system, there is a double-reflection (reflection from first one, then the other surface of the lens) ghost focus that is hazardous over about 0.14 to $0.16 f$. For left to right beams, again, there is a triple-reflection lens surface ghost that focuses at about $0.084 f$. Even this weak a ghost can have a few millijoules of energy and cause damage if a component is very near the focus, or if antireflection coatings degrade. There are similar sorts of ghosts located near every lens in the system, and tracking their positions and behavior is a major task in the optical design.

Expanding beams from these ghosts can also flood the pinholes with light, giving rise to nearly collimated “pencil-beam ghosts” that propagate forward and backward through the system. Generally these are harmless, but they can cause damage if antireflection coatings are badly degraded.



Switchyard and Target Area Mirror System

The function of NIF's switchyard and target area (SY/TA) optical system (Figure 3) is to transport a set of 192 beams grouped into 48 quads from the laser to the final optics assemblies located on the target chamber. These quads are arrayed in cones pointing at target chamber center, with 24 on the top and 24 on the bottom of the chamber. The mirrors must provide sufficient clear aperture for incident beams and reflected diagnostic beams. The aim point of each quad, with respect to target chamber center, can move ± 30 mm transverse to the beamline and ± 50 mm along the beamline. The pointing is controlled by tilting mirrors, so the mirrors must have adequate aperture to accommodate the changes in beam position required for this pointing. Also, the

mirrors must be sized so that the beam can be centered on the frequency converters using mirror tilts. There are many other design drivers affecting SY/TA mirror sizes that originate elsewhere in the NIF design, such as beam spacing requirements at the final optics location, the requirement for target back-reflection diagnostics, and the line-replaceable unit (LRU) maintenance concept.

There could be as many as 17 distinct mirror types in the system, but it is very costly to have such a wide variety. Consequently, we have grouped the 816 SY/TA mirrors into nine types having similar size requirements and angles of incidence, as shown in Table 3. Each beamline has either four or five SY/TA mirrors, designated as LM4 through LM8; some beamlines lack LM6.

We set the size of these mirrors using a ray-trace analysis tool and a ProE CAD model. The models adjust the tilt of each mirror and determine the beam positions required to accommodate the desired range

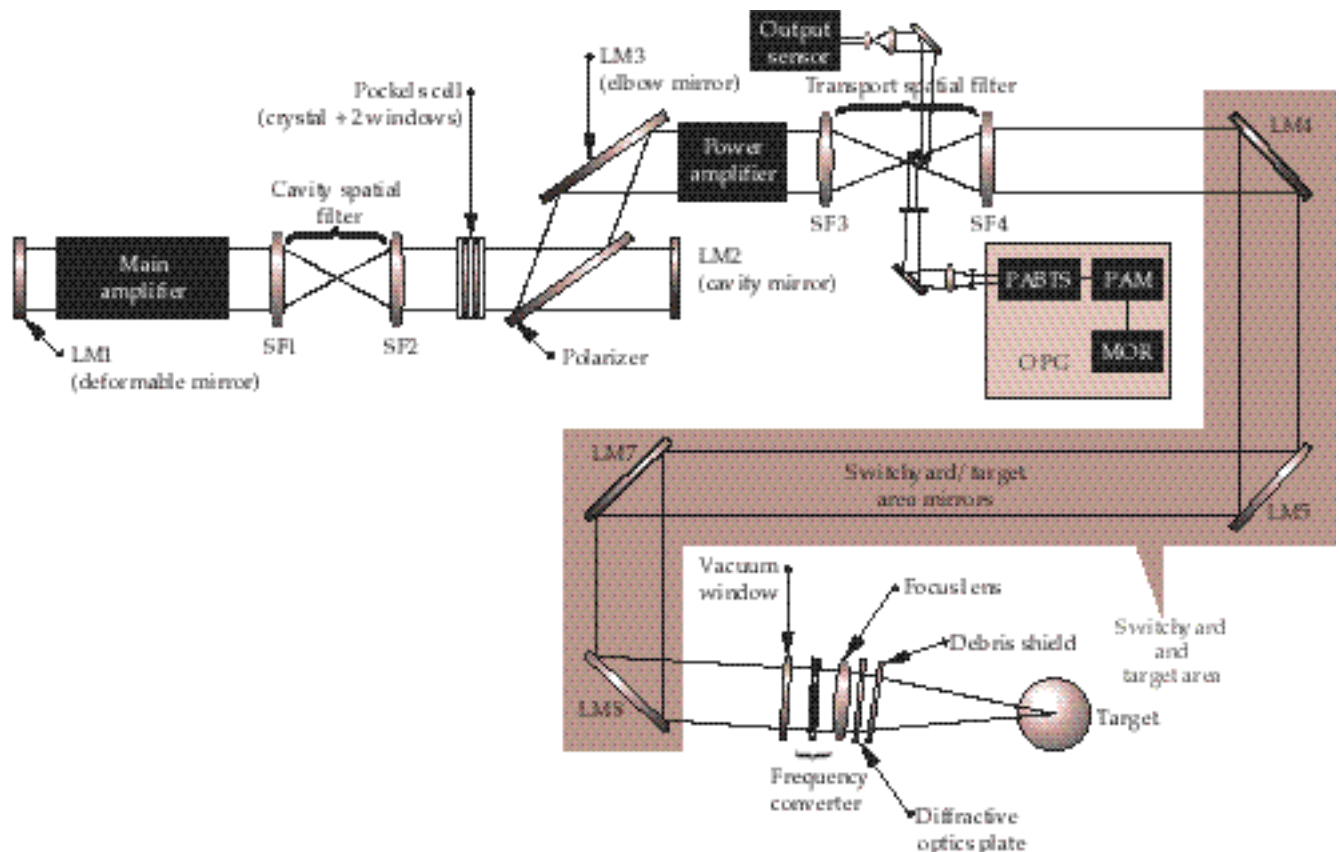


FIGURE 3. The switchyard and target area. (40-00-0997-2066pb01)

TABLE 3. Summary of switchyard/target area mirror characteristics.

NIF mirror position	Angle of incidence	Pol.	X-axis physical size and mechanical hard aperture (mm)	Y-axis physical size and mechanical hard aperture (mm)	Physical size diagonal (mm)	X-axis optical clear aperture (normal to optic) (mm)	Y-axis optical clear aperture (normal to optic) (mm)	Qty.
LM4A	45	S	507.0	595.4	782.0	477.0	565.4	96
LM4B	45	S	507.0	595.4	782.0	477.0	565.4	96
LM5	45	P	673.1	440.8	804.6	643.1	410.8	192
LM6	45	S	501.4	718.6	876.2	471.4	688.6	48
LM7A	14.1 16.9 19.7	S	502.0	524.6	726.1	472.0	494.6	48
LM7B	25.3 28.1 30.9	S	509.8	591.0	780.5	479.8	561.0	48
LM7C	36.6 39.4 42.2	S	503.2	688.0	852.4	473.2	658.0	96
LM8A	20.0 22.8	P	535.6	490.6	726.3	505.6	460.6	128
LM8B	30.0 33.2	P	586.2	483.2	759.7	556.2	453.2	64

of pointing and centering at the target chamber center and final optics assembly. Briefly, LM4 and LM5 move to center the beam on the final optics assembly. LM7 and LM8 move to compensate for any beam rotation in the path, and LM8 controls the final pointing to the target position. LM6, if present, does not have a control function. The ray-trace model quantifies the additional aperture required for each mirror to accommodate pointing the beam off-axis in the target chamber.

Title II Activities

For Title II, we will update the ray-trace model and the model that controls the optical configuration for the SY/TA mirrors to reflect a change in the final optics assembly focal length to 7700 mm. We will also develop a comprehensive model of the beam-lines to verify mirror sizes so that we can begin the procurement process.

Final Optics Assembly

The final optics assembly contains four integrated optics modules, one for each beam in a quad. Each module contains a vacuum window, two frequency-conversion crystals, a final focus lens, a diffractive optics plate, and a debris shield (Figure 4). The primary functions of the final optics assembly are to convert the laser light to 3 μm and focus it on the target (see “How Frequency Conversion Works” on p. 120). The system also smooths the on-target 3 μm irradiance profile, moves the unconverted light away from the target, and provides a vacuum barrier between the laser and the target chamber. The system also has two additional alignment and diagnostic functions: to provide a signal for frequency conversion alignment and to provide a signal for power and energy diagnostics.

A failure of the target chamber vacuum window could have severe consequences because of the high

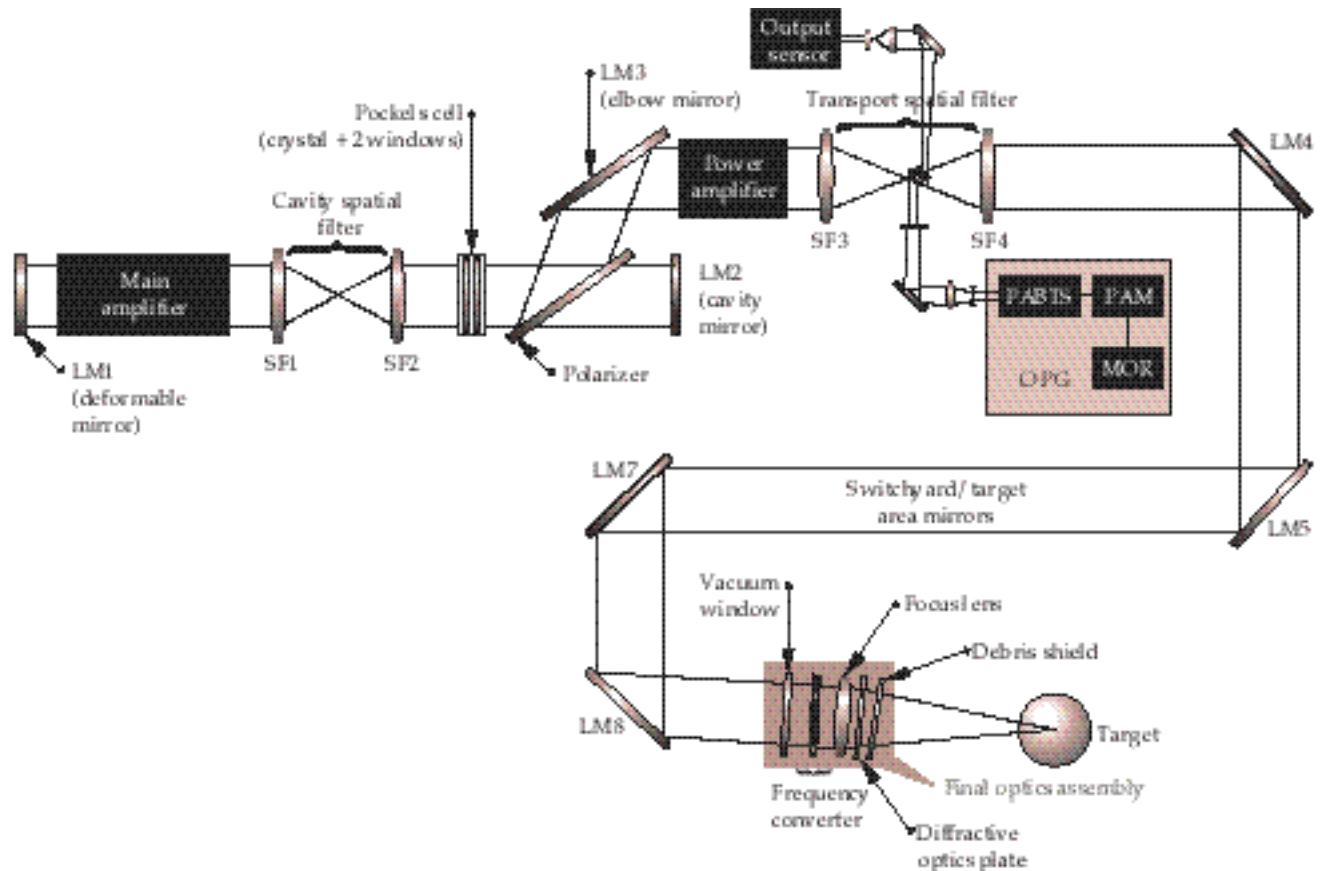


FIGURE 4. The final optics assembly. (40-00-0997-2067pb01)

value of the equipment in the target chamber and the possible release of tritium gas. Careful studies of fractured lenses on Nova show that a fused silica window will fail with no more than a single full aperture crack if designed to a peak tensile stress less than 500 psi. Therefore, we designed the NIF chamber window to that stress level. The window is thick enough (43 mm) that it would seriously limit the peak power on target if it were in the 3 beam, so the frequency converters and a thin 3 target focus lens must be placed in the vacuum environment of the target chamber.

The final optics cell, which holds and positions the two crystals and the focus lens, must have an optical clear aperture of 400×400 mm. Title I requires a focal length for the final focus lens of 7000 mm; this will be changed to 7700 mm early in Title II. This new focal length will allow each integrated optics module to be an individually removable LRU. The final optics must

divert the unconverted 1 and 2 light at least 3.0 mm from the center of the laser entrance hole (LEH) in an indirect-drive laser ignition target. (The unconverted light is diverted much more in the Title I design because of the use of diffractive optics, as discussed below.) The system must also provide for pointing the focused spot within ± 5 cm of target chamber center.

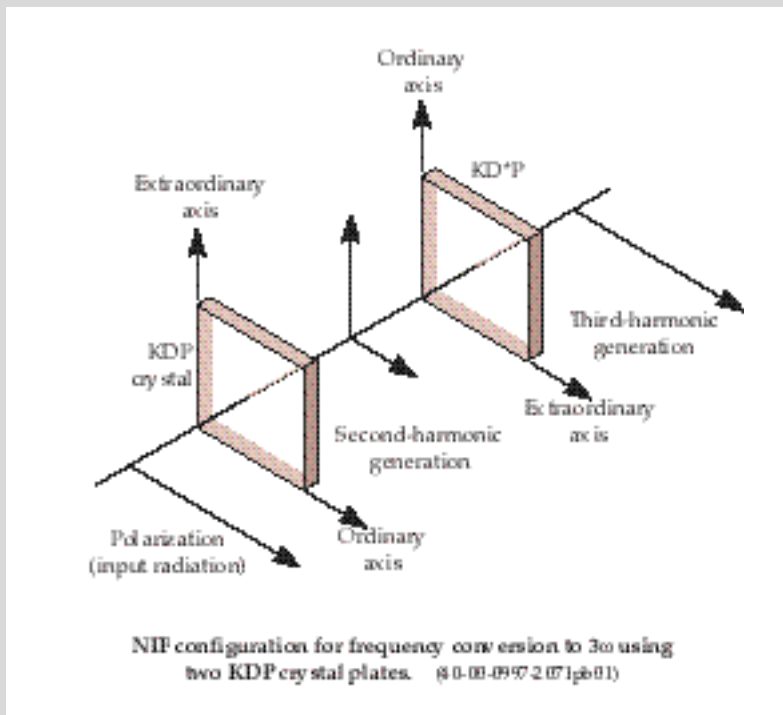
The major design drivers for this system are ghost reflections, damage, optics fabrication, flexibility for different user applications—such as direct-drive experiments—and beam control.

In the Title I design of the final optics, the frequency-conversion crystals and focus lens are mounted together in a final optics cell that allows tip-tilt adjustment for the crystals and translation to move the focal point in the target chamber. The plano-convex focus lens has its flat surface facing away from the target so that the flat first surface

HOW FREQUENCY CONVERSION WORKS

A neodymium glass laser like NIF generates light at a wavelength of about $1\ \mu\text{m}$ in the infrared region. However, we know that inertial fusion targets perform much better when driven with ultraviolet radiation. The NIF laser will convert the infrared ($1.05\ \mu\text{m}$ or $1\ \mu\text{m}$) light to ultraviolet (approximately $0.35\ \mu\text{m}$) using a system of two nonlinear crystal plates: one made of potassium dihydrogen phosphate crystal (KDP), the other of its deuterated analog, KD^*P . The figure shows the arrangement of the two crystal plates. The first plate converts two-thirds of the incident 1 radiation to the second harmonic ($2\ \mu\text{m}$) at $0.53\ \mu\text{m}$. Then the second crystal mixes that radiation with the remaining $1.05\text{-}\mu\text{m}$ light to produce radiation at $0.35\ \mu\text{m}$, or the third harmonic ($3\ \mu\text{m}$).

This process has a peak efficiency greater than 80%, and the efficiency can exceed 60% for the complex shapes used to drive ignition targets.



provides a back-reflected beam to alignment sensors and diagnostics located near the focal plane of the TSF. The lens also has a beam sampling grating for providing a diagnostic signal to an energy measurement calorimeter. The beam then goes through a separate diffractive optics plate, which contains a color separation grating and a kinoform phase plate. The grating moves the unconverted light well away from the target by creating multiple diffracted orders. The diffractive optics plate can be customized for various spot sizes and profiles, which provides flexibility for experiments studying indirect drive, direct drive, weapons physics, weapons effects, and other applications. The main beam and the diagnostic beam then pass through the debris shield, which is the last optical element in the system. This 10-mm-thick fused-silica optical element protects the final optics from target debris and

contamination. Table 4 shows the sizes and apertures for the final optics assembly (FOA) components. Some dimensions need to be verified by more detail design during Title II.

The exact relative positions of the optical components in the FOA are determined by careful analysis of the ghost reflections. The ghost analysis is complicated by the 12 surfaces involved, the mechanical restrictions in spacing the optical components, the requirement to accommodate a $\pm 5\text{-cm}$ focus adjustment, and the tolerances involved in fabricating the focus lens. We locate the window and debris shield where they are safe from damage, then tilt them to eliminate potential ghost problems (Figure 5).

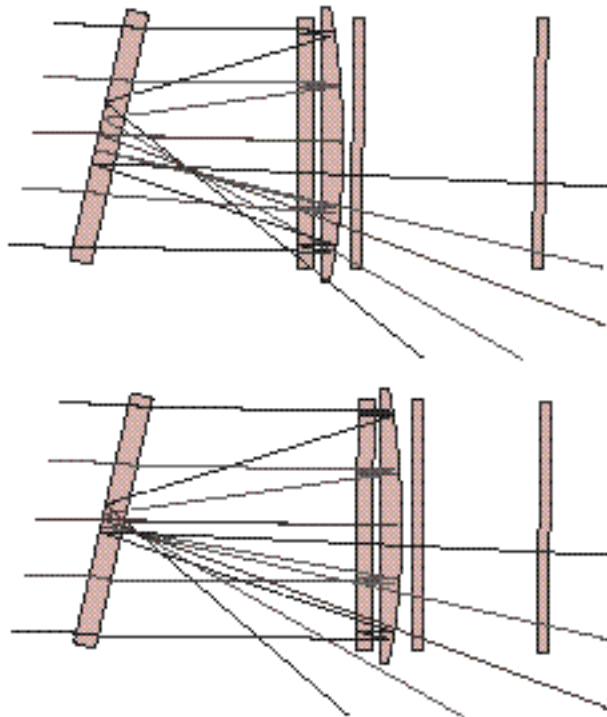
NIF uses a new color separation grating (CSG) technology for separating the $3\ \mu\text{m}$ light from unconverted $1\ \mu\text{m}$ and $2\ \mu\text{m}$ light. This grating allows the focus lens to be much thinner than it would be if refraction were

TABLE 4. Title I optics sizes and apertures for the final optics assembly.

Optic	Name	Optical clear aperture (mm)	Mechanical hard aperture (mm)	Optics size (mm)
Focus lens	FL	400 × 400	401 × 401	430 × 430 × 25
Doubler	SHG	400 × 400	400 × 400	410 × 410 × 11
Tripler	THG	400 × 400	400 × 400	410 × 410 × 9
Debris shield	DS	400 × 400	420 × 400	440 ^c × 420 × 10
TCvacuum window	TCVW	400 × 400	410 × 410	440 ^c × 440 ^c × 43 ^c
Diffractive optics plate	DOP	400 × 400	420 × 400	440 ^c × 420 × 10

^c Dimensions need to be verified in detail design during Title II

The window position is set by the lens triple-reflection ghost



Window and debris shield are tilted to help control ghosts

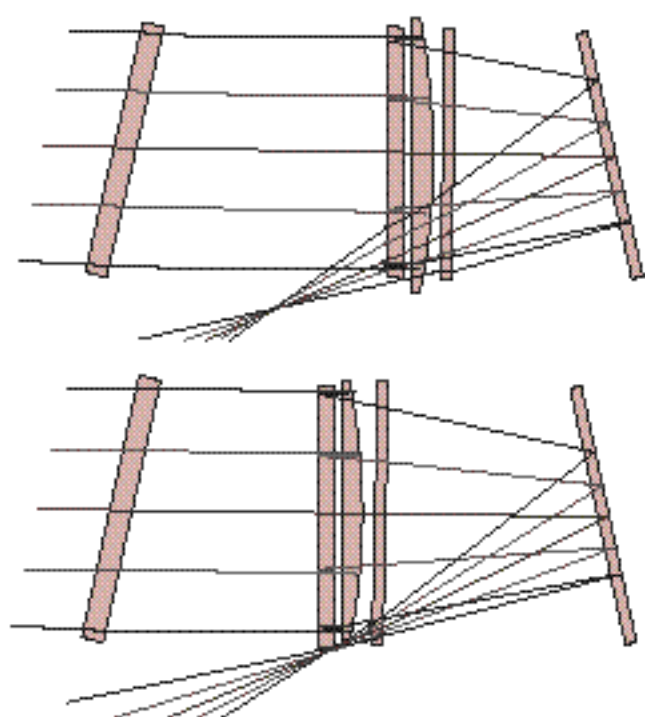
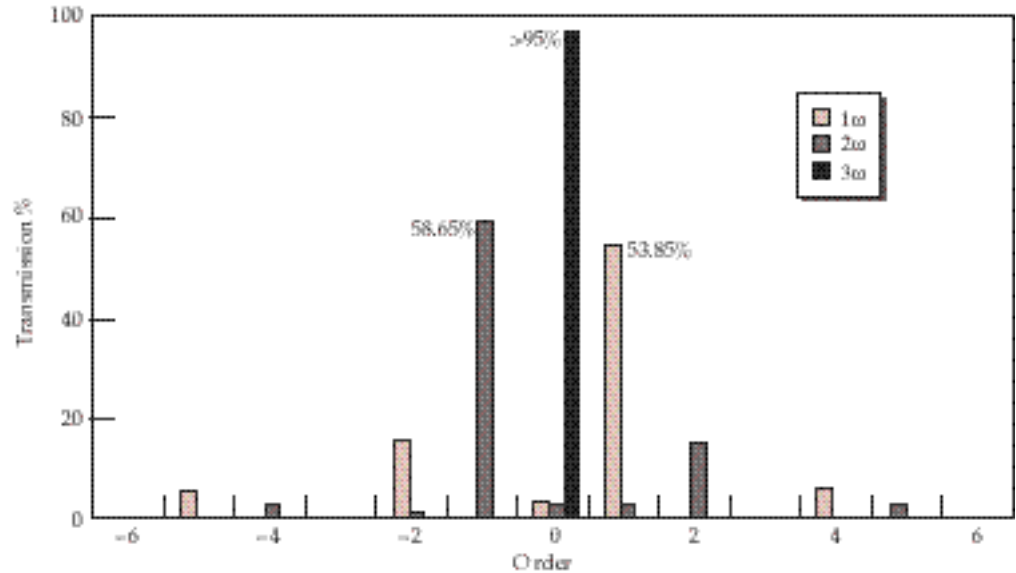


FIGURE 5. Ghost reflection analysis in the final optics. (40-00-0997-2068pb01)

used to remove unconverted light, as was done on Nova. The CSG is a kinoform or diffractive optic structure. On its surface are steps that have an optical path difference of exactly one wavelength at 3λ . These steps diffract the unconverted 1λ and 2λ light out of the beam. The pattern of these steps determines the

position of the unconverted light at target chamber center and on the opposite wall of the target chamber. A subscale (12-cm) CSG of this sort has been fabricated; it easily met the minimum NIF specifications for transmitting $>95\%$ of 3λ light and $<5\%$ of 1λ and 2λ light, to the zero order (Figure 6).

FIGURE 6. Color separation grating performance of a 12-cm part meets minimum NIF specifications. (40-00-0997-2069pb01)



Title II Activities

In Title II, we will complete the analysis to determine the dimensions of the vacuum window, the diffractive optics plate, and the debris shield. We will also verify our ghost management solutions by adding tolerances to our ghost analysis, finalizing window and debris-shield tilt angles, and specifying baffle and absorber locations. We will analyze the unconverted light distribution from the CSG and choose a design that optimizes the placement of unconverted energy both near the target chamber center and on the beam dumps on the opposite wall of the chamber. We will also finalize the kinoform design for user-defined NIF irradiance patterns.

Specifications for Large-Aperture Optics

Each one of the 7000 large-aperture optics in the NIF system must be manufactured by outside vendors. To be certain that we get optics that meet users' requirements at a minimum cost, we are producing a set of detailed specifications. We are iterating these Title I draft specifications with vendors to ensure that, with the final specifications, the optics can be manufactured and that they meet NIF performance requirements.

We divide the specifications into two basic types: optical quality specifications (wavefront error, transmission and reflectance, etc.) and design-related specifications (dimensions, radius of curvature of lenses, etc.). The optical quality specifications are derived using three techniques. First, we follow the flow-down of NIF requirements to ensure that we meet the primary criteria of the system. There are two general

optical requirements: the focal spot required on the target (1.8 MJ of 3rd energy within a 600- μ m-diam spot, and a goal of half the short-pulse energy within a 100- μ m spot), and the reliability, availability, and maintainability of each optic. We also derive the specifications empirically, tying the NIF design to historical results with Beamlet and Nova optics, thus ensuring the manufacturability of the optics. Finally, we determine measurement limitations, so that the requirements are interpreted in measurable terms. Below, we discuss several important optical quality specification areas: the wavefront error, which is dependent on spatial wavelength regions of varying scale, and discrete defects and coatings, which are independent of the spatial wavelength regions.

Wavefront Error

We define three spatial wavelength regions for wavefront error, where L is the spatial wavelength:

1. Figure, where $L > 33$ mm.
2. Waviness, where 33 mm $> L > 0.12$ mm.
3. Roughness, where $L < 0.12$ mm.

These regions have different effects on the beam, and are discussed separately below.

Figure

We further divide the figure error into three bins based on the ability of the deformable mirror to correct them. Models for the mirror show that it corrects 99% of 0–0.5 cycle error ($L > 800$ mm), 90% of 0.5–1.5 cycle error (800 mm $> L > 267$ mm), and none of the 1.5–12 cycle error (267 mm $> L > 33$ mm). “Cycle” refers to cycles across the 400-mm aperture.

To determine the figure error of a particular element, we track the peak-to-valley (P-V) contributions from the following sources:

- Fabrication. We assume these errors are relatively small: 0.15 λ for crystals, and 0.2 λ for all other optics.
- Lens misalignments. We assume that a pair of lenses can be aligned to a total wavefront error of 0.25 λ of focus, and that the angle tolerance on SF1/SF2 can create 0.2 λ of coma. Slight mirror, crystal, or slab misalignments will not affect the wavefront.
- Coating. For mirrors and polarizers, we specify a total reflected wavefront error of 0.3 λ at 1 μm , for both fabrication and coating.
- Thermal effects. Thermal effects are mainly present in the amplifier slabs, due to instantaneous flashlamp loading and residual temperature gradients. We assume the cumulative effect in the slabs is about 5 λ .
- Environment. Coatings respond to changes in humidity, so we are restricting the humidity fluctuations in the laser to those that create <0.125 λ wavefront error.
- Structural effects. We assume that the gravity sag from transport mirrors is 0.2 λ , and that mounting errors for the transmissive elements are negligible, except for the amplifier slabs at 0.1 λ .

We add errors coherently according to how many times the laser beam passes through an element, and add errors incoherently according to the number of elements involved. For example, if the fabrication error for a cavity lens is 0.1 λ , and two cavity lenses are multipassed four times, then wavefront error² = 2(4 \times 0.1 λ)², or wavefront error = 0.566 λ .

This analysis shows that the wavefront error in the “figure” spatial frequency range is dominated by pump-induced thermal distortions in the amplifiers. Also, fabrication errors could be relaxed from $\lambda/6$ to $\lambda/3$ without significantly affecting the total wavefront error. Alignment of the spatial filter lenses strongly affects the accumulated wavefront error. Finally, wavefront errors in the 1.5- to 12-cycle spatial frequency bin are the limiting factor in beam quality and focusability, since they are not corrected but are transmitted through the spatial filter pinholes, which cut off errors at shorter spatial wavelengths.

Figure errors are specified in three ways, namely the P-V wavefront error (the value of $\lambda/3$ discussed above), the rms wavefront error (which is usually derived from the P-V error), and a wavefront gradient limit. The gradient limit is used to control the short spatial wavelength region (267 mm $>$ L $>$ 33 mm) that contributes to the minimum focal spot size. A gradient specification of ($\lambda/90$)/cm, or (equivalently) 99.8% of

slope errors $<$ ($\lambda/30$)/cm, will allow us to meet NIF focal spot requirements. The wavefront error budget will be examined and reviewed in even greater detail early in Title II.

Waviness and Roughness

Errors in the “waviness” spatial frequency range (33 mm $>$ L $>$ 0.12 mm) cause irradiance noise on the beam. This noise can also seed the growth of irradiance noise due to the nonlinear index of refraction at high irradiance, and can ultimately lead to beam breakup and filamentation. Errors in this range are reset to zero every time the beam passes through a spatial filter pinhole, at which point they constitute an optical loss.

Errors in the “roughness” range (L $<$ 0.12 mm) are not as dangerous for seeding nonlinear growth, except for 3 μm optics where seeding of filamentation is important for L a bit smaller than 0.12 mm. Roughness also leads to an optical loss.

We specify waviness and roughness using a not-to-exceed line on a power spectral density (PSD) plot of the optical surface (Figure 7). Tests on many Beamlet and other parts show that the specification shown here is achievable with good manufacturing practice, and will be reasonable for NIF.

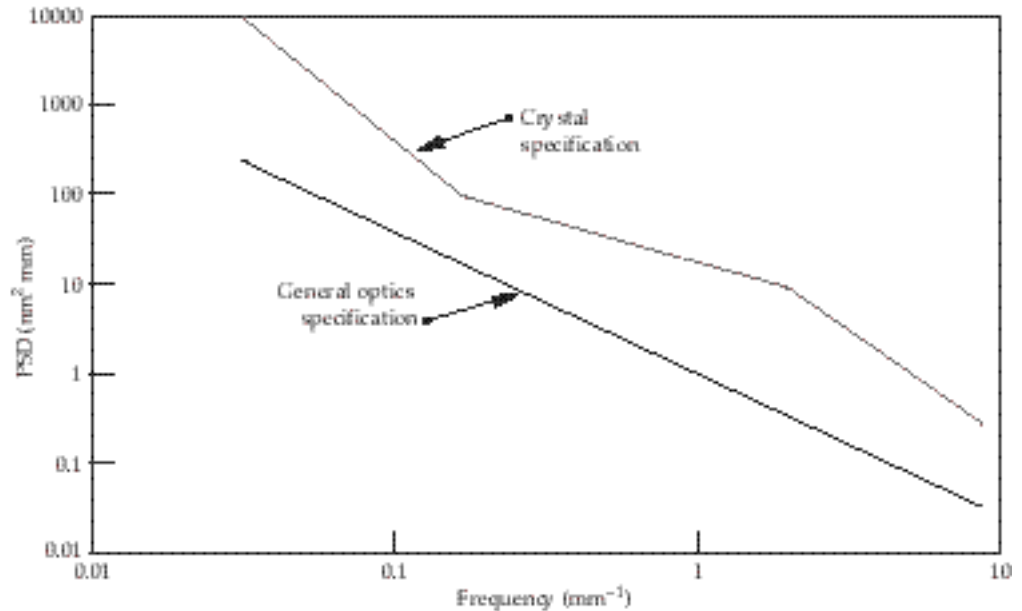
Discrete Defects

All optical components contain discrete defects, such as bubbles, inclusions, and scratches. These may lower the damage threshold of the part, and a high concentration of defects can lead to noticeable optical losses. We specify discrete defects using the ISO 10110 standard that is beginning to be used for optical specifications.

Our preliminary specification for defects such as bubbles is 26 \times 0.25, which in ISO notation means less than 26 defects each having a maximum area of (0.25 mm)². Any number of smaller defects are allowed by the standard, so long as the total obscured area does not exceed 26 \times (0.25 mm)². Opaque inclusions generally lead to very low damage threshold, and are not acceptable unless it can be demonstrated that they will not damage at NIF operating fluence. The scratch/dig specification is 100 \times 0.125. The long scratch specification is L1 \times 0.03 with a maximum length of 50 mm, where L designates “long,” 1 is the number of scratches allowed, and 0.03 is the width of the scratch in mm. Thus, one 30- μm -wide scratch 50 mm in length is allowed (or any combination of narrower scratches that total less than 30 μm width and are shorter than 50 mm).

We expect to refine these specifications in Title II based on further propagation analyses and experiments on damage initiated by defects.

FIGURE 7. Power spectral density specifications assure NIF performance.
(40-00-0997-2070pb01)



Coatings

Except for the amplifier slabs, all NIF optics have either antireflection coatings (lenses, crystals, and windows) or highly reflecting multilayer dielectric coatings (mirrors and polarizers). The antireflection coatings are deposited by a liquid-dip sol-gel process developed at LLNL. They have high damage threshold and, when new, have a transmission of 0.999 per surface at 1 μm and 0.998 per surface at 3 μm . There is some degradation with age.

Mirror and polarizer coatings are supplied by commercial vendors. We specify a reflectivity >0.995 for mirrors. Transport mirrors (LM4–LM8) must also have a reflectivity between 0.25 and 0.71 at 2 μm , and between 0.31 and 0.71 at 3 μm . There are a few other specialized specifications on transmission for some mirrors. Polarizers are specified to have an *S*-polarized reflectivity >0.99 and a *P*-polarized transmission >0.98 at a use angle of $56 \pm 0.5^\circ$ with a bandwidth of 1 $^\circ$.

Title II Activities

Design-related specifications are contained and controlled in our configuration drawings. As part of the Title I reviews, we have completed 82 large-aperture

drawings for blanks, finished parts, coatings, etc. The drawings exceed normal Title I standards and include mounting and handling details as well as detailed notes on the specifications. We are now ready to solicit procurement bids for those optics that require a long lead time.

In the optical specifications area, our list of Title II activities contain no critical items. Propagation modeling efforts will provide us with more detailed justification for specifying the rms gradient, PSD limits, and discrete defects for the various optics. Damage experiments could change the specifications for some discrete defects. Design engineers will be providing updates on mounting requirements, part sizes and so on, and vendors will be commenting on our assumptions in the wavefront error budget and providing general feedback on our drawings. We will incorporate the responses from design engineers and vendors as the design and specifications evolve. Another Title II priority is to develop supporting documentation on handling, inspection, and testing.

For more information, contact
R. Edward English, Jr.
Opto-Mechanical Systems Engineer
Phone: (925) 422-3602
E-mail: english2@llnl.gov
Fax: (925) 424-6085